KERNFORSCHUNGSZENTRUM

KARLSRUHE

May 1970

KFK 1201
IAEA-CN-26/113

Institut für Angewandte Kernphysik

Neutron Total, Scattering and (n, x) Reaction Cross Sections above the Resonance Region

S. Cierjacks

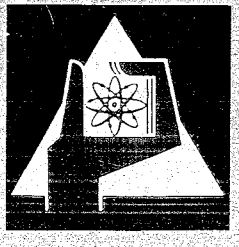

GESELLSCHAFT FÜR KERNFORSCHUNG M. B. H.

KARLSRUHE

KERNFORSCHUNGSZENTRUM KARLSRUHE

May 1970

KFK 1201
IAEA-CN-26/113

Institut für Angewandte Kernphysik

Neutron Total, Scattering and (n,x) Reaction Cross Sections above the Resonance Region

S. Cierjacks

Gesellschaft für Kernforschung mbH., Karlsruhe

Abstract:

In this review talk the present status of neutron facilities used for fast neutron cross section measurements is condidered. A few topis are then discussed in some detail. In the important area of total neutron cross sections, several examples of new high resolution data are shown. Comparisons of other data with optical model calculations are also considered. Scattering cross section measurements are reviewed and the sphere transmission method, associated γ-ray method and time-of-flight method are discussed. Finally the area of (n,x) reaction cross sections is briefly reviewed. Concluding remarks are made concerning the accuracy of presently available data.

Zusammenfassung:

In diesem Bericht wird eine Übersicht über den gegenwärtigen Stand der Messungen von Neutronenwirkungsquerschnitten und der verwendeten Experimentiereinrichtungen gegeben.
Im einzelnen wird auf totale, Streu- und Reaktionswirkungsquerschnitte eingegangen. Es werden mehrere Messungen hoch aufgelöster totaler Neutronenwirkungsquerschnitte angeführt. Die gemittelten Daten werden mit Rechnungen nach dem optischen Modell verglichen. Für die Messung von Streuquerschnitten werden verschiedene Methoden diskutiert. Im einzelnen wird auf die Flugzeitmethode, die Methode der assozierten γ-Strahlung und die Kugeltransmissionsmethode eingegangen. Es wird ebenfalls das Gebiet der (n,x) Reaktionen betrachtet. Abschließend wird die Genauigkeit der verfügbaren Neutronenwirkungsquerschnittsdaten diskutiert.

INTERNATIONAL ATOMIC ENERGY AGENCY
SECOND INTERNATIONAL CONFERENCE ON NUCLEAR DATA FOR REACTORS

15 - 19 June 1970

Helsinki

IAEA-CN-26/113

NEUTRON TOTAL, SCATTERING AND (n,x) REACTION CROSS SECTIONS ABOVE THE RESONANCE REGION

S. CIERJACKS

INSTITUT FÜR ANGEWANDTE KERNPHYSIK
KERNFORSCHUNGSZENTRUM KARLSRUHE
F.R. GERMANY

1. INTRODUCTION

It is a well known fact that the threshold of the range above the resonance region means different energies according to the nuclei considered. The beginning of this region may be above several MeV for light nuclei but can also be reached at about several keV in the heavy mass region. In addition there is no well defined energy which separates the two regions one from the other. Rather there is an intermediate range in which individual levels become more and more overlapping. We shall take the energy region which is of interest here to mean the range between about 100 keV and 10 MeV and refer to it in addition as the fast neutron region.

This area of cross section measurements is a very large one and numerous groups are engaged in it. Therefore none of the listeners should expect that I could cover this field in half an hour. Preparing this talk, I had to choose between the two possibilities either to touch as much experiments as possible very briefly or to discuss only a few points in some detail. I decided in favour of the last choice although I feel quite unhappy in view of the numerous contributions offered to me on request

by various groups from many countries. Furthermore it seemed proper at this conference to give primary attention to experimental and applied aspects of fast neutron cross sections and not to the physical interpretation of the cross section behaviour.

With this intent, the talk will concentrate on the following topics: Present neutron facilities used in the fast neutron region, measurements and some interpretation of total, (n,x) and scattering cross sections. Finally a few remarks concerning the accuracy of available data will be added.

2. NEUTRON FACILITIES USED FOR FAST NEUTRON CROSS SECTION MEASUREMENTS

The facilities presently used for cross section measurements above the resonance region can be divided into two main groups according to the neutron sources involved.

1. Facilities using charged particle rections with light nuclei to produce nearly monoenergetic neutrons, such as Li^7 (p,n) Be^7.
2. Devices which produce wide continuous neutron spectra by interaction of high energy electrons or charged particles with mainly heavy nuclei.

Van de Graaff accelerators and Cockcraft-Walton machines belong to the first category of devices. Those can be operated either in the continuous or the pulsed beam mode. In the following, we will only consider the latter application since this is favoured in most cases for fast neutron cross section work. Van de Graaff accelerators with top terminal pulsing and pulse compression systems can be used to produce pulses of about 10 mA of protons with 1 nsec duration. Several machines with 3, 5, 6 and 8 million volts are in use. In general monoenergetic neutrons in the energy region between 0.1 - 10 MeV are produced by the following reactions:

Li^7(p,n) Be^7	between	$0{,}1 \leqslant E_n \leqslant 0{,}6$ MeV	with $Ep \leqslant 2{,}25$ MeV
T (p,n) He^3	"	$1{,}5 \leqslant E_n \leqslant 4{,}5$ "	" $Ep \leqslant 5$ "
D (d,n) He^3	"	$4{,}5 \leqslant E_n \leqslant 10$ "	" $E_d \leqslant 8$ "

where the projectile energies correspond to neutron observation in the forward direction.

Of course each of these reactions may also be used to produce higher energy neutrons as indicated here but in typical monoenergetic neutron experiments there arise some complications because of (i) the second neutron group in the Li(p,n) reaction above Ep $\approx$ 2,25 MeV, (ii) the secondary processes in the T(p,n) reaction above Ep $\approx$ 5 MeV and (iii) the deuteron break up processes in the D(d,n) reaction above $E_d \approx 8$ MeV: The optimum energy resolutions which could be observed in some experiments with monoenergetic neutrons are 1 - 2 keV, 2 - 5 keV and 20 keV, respectively, in the above three regions.

Most of the devices using linear accelerators, proton or deuteron cyclotrons as pulsed neutron sources have been utilized in the field of fast neutron cross section measurements only for a few years. Nevertheless a tremendous amount of total cross sections have already been determined with these facilities. Electron linear accelerators provide neutron bursts of 5 - 10 nsec duration and a time averaged neutron intensity of up to $\sim 10^{14}$ neutrons/sec [1], proton and deuteron cyclotrons bursts of 1 - 3 nsec duration and a time average neutron intensity of up to $\sim 2 \cdot 10^{14}$ neutrons/sec [2] which allow high resolution and precision time-of-flight measurements using flight path lengths of typically 200 m. The resulting energy resolutions show the well known $E^{3/2}$-dependence. With the electron linac at GGA Carlson [3] has obtained energy resolutions ranging from 0.3 keV at 500 keV to ~ 30 keV at 10 MeV. With the new 190 m flight path installed at the Karlsruhe isochronous cyclotron the corresponding energy resolutions obtained so far range between 0.2 keV and 20 keV. Excluding the subject of energy resolution which may not be the critical point at all, it should be clear that these continuous spectra type facilities combine the advantages of extremely high neutron intensities and broad neutron spectra.

With some of these facilities [1,2] neutron fluxes even at the end of a 200 m flight path are up to 3 - 4 orders of magnitude higher than those obtained with Van-de-Graaff accelerators in a distance of 1 m from the target, if an equivalent energy spread of the neutrons from a monoenergetic source is taken into account. This fact is advantageous mainly for (n,x) and scattering cross section measurements which were stimulated at some laboratories some time ago and which just now have shown some first results [4,5].

In Fig. 1 three typical neutron spectra are shown which have been obtained with the RPI 140 MeV electron linac (a), with the 140 MeV proton synchrocyclotron at Harwell (b), and the Karlsruhe isochronous cyclotron (c) [6]. All intensities are given in relative units.

3. TOTAL NEUTRON CROSS SECTIONS

The measurements of total neutron cross sections are in principle reasonably easy to perform, because the transmission method does not require a determination of the neutron flux from the source.+ Most of the measurements of total neutron cross sections are made with proton recoil detectors though there are some exceptions [7,8]. In fig. 2 the geometry of the time-of-flight facility used with the Karlsruhe isochronous cyclotron is shown. This arrangement is used for total neutron cross section measurements in the region from 0.5 - 32 MeV. Neutrons are detected with a 25 cm Ø, 1 cm thick plastic scintillator. For beam monitoring, a small liquid scintillator is placed at an angle of - 6° to the main flight path. The neutron beam is suitably collimated by two collimators inside the vacuumtube of 1 m diameter. Similar arrangements are used on other neutron time-of-flight spectrometers.

A recent remeasurement of the total neutron cross section of oxygen at Karlsruhe using the new 190 m flight path is shown in fig. 3. These data clearly illustrate the presence of separated resonances, typical of the light nuclei in the MeV region. In addition to the well known broader resonances these new measurements show several narrow resonances which either have not been seen or not fully resolved in the measurement with the 60 m flight path. Among these are also some which were seen previously only in other reactions. This is true for instance for the level at 1,690 and the level at 3,007 MeV, with widths smaller than 0,5 and 1,5 keV. (Only the energy region between 3-7 MeV is shown).

As an example of a medium weight nucleus fig. 4 shows some excellently resolved cross section data of iron from a measurement of Carlson and coworkers at GAA [9]. At 500 keV this nucleus still shows isolated resonances with widths comparable to the level spacings. With increasing energy we can observe more and more overlapping of levels.

+Nevertheless some kinds of difficulties arise in high resolution and high precision measurements from either the determination of the absolute energy scale [10], of inscattering effects or dead-time considerations [11].

To investigate the presence of intermediate structure for several medium and heavy weight nuclei, Carlson and Barschall [12] measured the cross sections of 18 elements from Mg to Bi in the region between 4,5 and 14 MeV with high resolution and precision. Their results for S are shown in fig. 5. All fluctuations found in this energy region for some medium weight nuclei could be explained satisfactorily in terms of statistical fluctuations of the level widths and the level spacings.

Cabé et al. at Saclay measured total neutron cross sections for some light and medium weight nuclei from 0,4 - 1,2 MeV [13, 14]. Fig. 6 illustrates their results obtained for iron. In addition to the fine structure (fig. 6a) which arises from the many resonance states of the compound nucleus, there is seen a phenomenon known as "intermediate structure" (fig. 6b). This structure having spacings of ~ 200 - 300 keV and widths of about 50 - 100 keV is reported to result from the initial formation of simple compound nuclear states such as (2p, 1h)-states. Though structure of this type has been observed in the scattering cross sections of several elements [15] so that its existence is not questioned, some care must be taken in the interpretation considering only the total cross sections. Therefore, I will come back to this topic in the discussion of the neutron scattering data.

Fig. 7 illustrates some moderately resolved data from a variety of 78 naturally occuring elements and 14 separated isotopes obtained by Foster and Glasgow [16] in the energy region between 3 and 15 MeV. The large body of data observed under identical experimental conditions have been used to check the predictions of the nonlocal model of Perey and Buck [17]. The solid circles in this figure demonstrate a seven point sliding average of the original data. The solid curves are obtained from optical model calculations. Good agreement between the experiments and theory is observed for spherical nuclei (only some are shown). However, the experimental results systematically deviate from the predictions for highly deformed nuclei. This result supports the previous assumption, that the spherical nonlocal optical potential should adequately describe the energy variation of σ_T for spherical nuclei, but yields less accurate results in the region of high deformation.

Unfortunately the above conclusions can not be extrapolated to the regions of lower or higher energies. At Karlsruhe we have just finished a similar analysis for a variety of 19 elements and 1 separated isotope in the extended

region from 0.5 - 32 MeV [18]. Some of our results are shown in fig. 8. It can be seen from this figure that the agreement between the experiment and the theory mainly below 3 MeV but also above 20 MeV is less satisfactory also for spherical nuclei. This result is in accordance with the observations made for neutron scattering cross sections near 1 MeV [19 - 22], where the data cannot be matched with this potential. In this region, good agreement could however be obtained with the Moldauer potential [23].

It was recently reported [24], that the total n,p scattering cross section show small but statistically significant oscillation in the energy dependence. This has stimulated some new high precision cross section measurements in the fast neutron region. As an example the results obtained by Schwartz et al. at NBS [25] are illustrated in fig. 9. In accordance with the results of some other laboratories [26-28] no significant structure was found.

4. NEUTRON SCATTERING CROSS SECTIONS

A large amount of accurate fast neutron scattering data have been measured during the last few years [28-34]. These data range in the total energy region between about 0.1 - 10 MeV though there is an overwhelming portion in the region below 1.5 MeV. There are two important reasons to acquire scattering cross section data: The accurate knowledge of fast neutron scattering cross sections (i) is essential for the design of advanced nuclear reactors and (ii) allows the predictions of suitable nuclear models to be checked. Having such models gives not only better understanding of nuclear reactions, but also provides the reactor physicists with a tool to calculate unknown cross sections.

There is a lot of techniques used for the fast neutron scattering cross section measurements. Only three of the most important methods should be mentioned:

1. The sphere transmission method

This is a very elegant method to determine the nonelastic cross sections which often are equivalent to the inelastic scattering cross section. The essential point in this method is the self cancellation of the elastic scattering from all portions of the sphere shell surrounding either the source or the detector. The observed transmission of this shell can be

simply related to the nonelastic scattering cross section. The application of this method, however, is limited by the spectroscopic quality of the detectors and the possibility to determine complex correction factors..

2. The associated γ-ray method

This method deals with the registration of γ-rays emitted during the deexcitation of the residual nucleus formed by fast neutron scattering reactions. It can be used to determine accurate γ-ray production cross sections, which often can be related to the neutron inelastic scattering cross sections. If Ge (Li) detectors are used, relative intensities, energy and angular distributions for all occurring γ-transitions can be determined very accurately from a single experiment. With the exact knowledge of these quantities the inelastic scattering cross section can be derived from these measurements if there is no transition of the secondary neutrons to the continuum of the residual nucleus. But, this condition holds for a variety of light and medium weight nuclei up to several MeV incident neutron energy.

3. The fast neutron time-of-flight method

Most of the presently available elastic and inelastic scattering cross section data have been determined by this method. An example of a neutron time-of-flight facility used in this field is shown in fig. 10 [35]. The arrangement consists of a pulsed monoenergetic neutron source, in this case a Van-de-Graaff accelerator. The scattering sample is placed close to the neutron producing target. The energies of the scattering neutrons are determined by the time-of-flight between the scatterer and the neutron detectors positioned at several angles around the scatterer.

Fig. 11a gives an example for a measurement done with the latter type of apparatus. This figure shows elastic and inelastic neutron scattering cross sections obtained for vanadium which were measured by A.B. Smith at Argonne [35]. At the left, the experimental total neutron cross sections, total elastic scattering cross sections (lower part) and the first five Legendre polynomial coefficients obtained from a least squares fit to the angular distribution measurements (upper part) are illustrated. Fig. 11b contains the measured inelastic scattering cross section for the excitation of the 0,32 and the 0,93 MeV levels of ^{51}V. All observed cross sections are characterized by both, a fine and an intermediate energy dependent structure. The intermediate structure can be described by a width and a spacing large compared to that of compound nuclear states, but small relative to that of the single particle or diffraction "giant resonances".

The observed structure in the elastic and inelastic channels were found to be correlated in scattering angle. Structure of this type can be interpreted in terms of doorway state processes such as mentioned in the preceding section. To reproduce not only the smooth energy dependence but also the observed structure, the authors analyzed their data with an intermediate optical potential. This potential has been interpreted to be a conventional optical potential modified only by the presence of two energy dependent factors classifying a limited number of doorway states. Each of these is characterized by its resonance energy, a decay width of the doorway to the compound nucleus and a strength of the interaction with the doorway. The adjustment of the parameters needed for a general application of such a potential was accomplished by a detailed fit to the measured elastic distribution restricting the number of doorway states to $\leq$ 5/MeV. The resulting intermediate potential was then used to calculate elastic and inelastic distributions for direct comparison with the measured values. The results of calculation were in qualitative agreement with the experimental results (comp. fig. 12). A wider application of this method may become a useful tool in the determination of statistical properties of doorway states.

Other large bodies of data have been obtained by Holmquist and Wiedling and coworkers at Studsvik /36/ and by Tsukada at Tokai-mura /29/. These two groups investigated the elastic and inelastic neutron scattering for a variety of nuclei in the region between 1.5 - 8 and 0.5 - 8 MeV, respectively, with an experimental arrangement similar to that shown in fig. 10. New results and the analysis of the data from these two groups will be presented in this session and, therefore, should only be mentioned here.

One example of the use of a Ge(Li) detector in the fast neutron inelastic scattering studies is given in fig. 13 a. This figure is from a recent publication of Roger et al. /37/ and shows the excitation function for neutron inelastic scattering to the 367 keV level in ^{45}Sc. The corresponding decay scheme of the residual nucleus obtained simultaneously from the measurement is shown in fig. 13b. The excitation function in fig. 13a was obtained by summing the γ-ray production cross section for the 364 and the 376 keV levels, since no cascading transitions to this level were observed. In a similar manner these authors determined the excitation functions for the inelastic scattering to six other levels up to 1412 keV. In some cases, e.g. for the level at 544 keV, the

cascading contributions from higher levels had to be subtracted.

With the knowledge of the angular distribution of the γ-rays which were taken from other experiments the excitation functions for several inelastic channels were obtained from the γ-ray production cross sections by correcting for cascading transitions.

A fascinating aspect in this context is the application of the associated γ-ray method to continuous spectra type pulsed sources which was recently demonstrated by Carlson et al. at GGA [4]. Their experimental arrangement is shown in fig. 14a. The use of the 140 MeV electron linear accelerator as pulsed neutron source allows to measure simultaneously the γ-ray production cross section in the total energy range from the threshold up to 15 MeV in a single run. The γ-ray energies and intensities are measured using a Ge(Li) detector and the corresponding neutron energy is determined by time-of-flight in a two-parameter experiment. First results for O were obtained at a backward angle of 125° using a ring sample (fig. 14b). The installation of a similar arrangement is nearly completed at the Karlsruhe isochronous cyclotron.

5. (n,x) REACTION CROSS SECTIONS

Neutron induced charged particle reactions such as (n,p) and (n,α) reactions and (n,2n) reactions are mainly threshold reactions and have been used for neutron flux determination as well as for neutron spectra measurements. These applications and nuclear structure studies are the main reasons that it is desirable to have detailed and accurate data of those cross sections from the threshold up to more than 10 MeV. While there is a large amount of data centered around 14 MeV [38-43], only comparatively few measurements have been made in the region below. The measurements of threshold reactions in this range often suffer from a lack of neutron intensity.

Most of the available data have been obtained by use of the activation technique. Activation measurements have two advantages: first, that large quantities of sample material can be used and second, that the constituent isotopes of an element can be distinguished. The disadvantage of this method is obvious. Such measurements yield the excitation functions only. If more detailed informations such as angular and energy distributions of the reaction products are wanted either the nuclear emulsion technique or direct counting of the emitted particles are necessary. For (n,p) and (n,α) reactions both methods deal with extremely small amounts of target material and only a few

of such measurements could be done in some favourable cases [44,45].

An experiment belonging to the latter category, was recently reported by Grimes [44]. Some of his results are shown in fig. 15. (n,α) and (n,p) reactions cross section were obtained for the favourable case of Si, where the silicon could serve as the scattering sample as well as the detector. Excitation functions have been determined for some separated α- and proton-groups characterizing the decay of the compound nucleus into some of the first low lying levels in ^{25}Mg and ^{28}Al, respectively.

In the same context, I would only mention some recent measurements of the (n,α) reaction cross section of ^{9}Be done at Karlsruhe by Kropp et al. [5]. Using the isochronous cyclotron as a pulsed source of fast neutrons gave reasonable intensity to measure double differential cross sections in a four parameter time-of-flight experiment with good sensivity and resolution. These first results promise that the continuous spectra type facilities may become a very powerful tool for the measurement of detailed (n,p) and (n,α) reaction cross sections in the near future.

In the high energy region the measured cross sections include not only data obtained at ~ 14 MeV, which were carried out with Cockcroft-Walton accelerators. For several measurements between 1 - 20 MeV Van de Graaff accelerators operated in the continuous beam mode have also been employed [45-48]. In this case neutrons were produced additionally by the DT-reaction. In fig. 17 two examples are given of energy dependent cross section measurements of threshold reactions between 1 - 20 MeV. One is that of the $^{60}Ni(n,p)$ reaction taken from a report of Paulsen [43] the other is the Al^{27} (n,α) reaction measured by H. Schmitt et al. [46] at Oak Ridge. From an examination of the cross section fluctuations in Al it can be seen, that it is necessary to take data at energy intervals smaller than the energy spread of the incident beam, if the true avarage energy dependence of the cross section is to be obtained.

With respect to new $^{10}B(n,\alpha)^{7}Li$ reaction cross section measurements a recent report of L. Steward at Los Alamos should be mentioned [49] in which the results from four laboratories are compared. This comparison (fig. 16) contains the results of Nellis et al. at TNC, who observed the γ-rays from the $^{10}B(n,\alpha\gamma)$ reaction and obtained an absolute cross section via a flux measurement using the hydrogen scattering cross section. Measurements by Davis et al. and Macklin and Gibbons are included along with Bogart and Nicols results. The comparison shows trends between the different sets of data. The author mentions,

that a renormalization of the Davis results would bring all data in agreement with the exception of Macklin and Gibbons results, which are based on the inverse reaction.

In addition to the observation of systematic trends found in (n,p) and (n,α) reactions [50], Chatterjee recently observed some similar effects for (n,2n) reactions [51]. The observation of systematic trends in those reactions can be of great importance to calculate unknown threshold reaction cross sections which are of interest for different kinds of reactor and engineering applications, and therefore will be discussed briefly. In the above publication Chatterjee plotted available (n,2n) reaction cross sections at three selected excitation energies versus the mass excess $(N-Z)_R = 2\zeta$ of the residual nucleus. This is shown in fig. 18 which contains the data in the mass excess range from 0 - 30 and for the excitation energy of U = 6 MeV. A gross trend curve A can be drawn through the most abundant target elements. At least three distinct minima shown as dotted curves are stemming out of the trend A which positions are roughly labelled as A_1, A_2; A_3, A_4 and A_5, A_6 corresponding to the values of 2ζ = 10, 14, 24. In addition remarkable effects are indicated by the weak solid straight lines and the dotted straight lines. The lines of constant N (residual isotones, weak solid straight lines) seem to align themselves approximately parallel to gross trend A. This trend, already known as Csikai Peto trend, shows that generally an isotone at lower residual Z value has a higher cross section than its higher isotopic member. Similarily there is the same trend for isotopes (dotted straight lines): a heavier isotope usually has a higher cross section than the lighter one. According to S. and A. Chatterjee all three trends can semiquantitatively be understood as a compound nuclear decay process where the available residual excitation of a suitably shifted Fermi gas is properly treated.

6. ACCURAY AND RELIABILITY OF PRESENTLY AVAILABLE DATA

The users of neutron cross section are interested primarily in obtaining accurate data for their research. Therefore, it should be fitting to this conference to add some remarks concerning the accuracy obtainable with the present capabilities of techniques and man power. A characterization of the accuracy and the reliability should include both, the typical uncertainties quoted for some advanced measurements and the comparison of various cross sections published in the literature. Of course, the comparision will be complicated by the effects of the different energy resolutions obtained in

different measurements. In these regions the comparison can be done only in those cases where the energy resolution has little effect.

In the case of total cross section data, the major portion of the more recent measurements have been carried out with a statistical accuracy of ~1 % for most of the data points. Absolute uncertainties additionnally must include errors due to background, inscattering or dead-time corrections. Typical quoted values for those measurements are 2 - 3 %. A comparison of total neutron cross section data, which have been collected in various previous compilations [52] often indicated the presence of systematic differences of several percent in the measurements from different laboratories. Many of the dicrepancies that did exist were gradually disappearing as measurements with better resolutions were superseding the older data. In addition several discrepancies vanished after some corrections were applied to a few data measured at Wisconsin [10] and at Karlsruhe [11]. A recalibration of the analysing magnet at Wisconsin caused a correction of their absolute energy scale. A careful reinvestigation of the dead-time introduced by the digital time analyser used with the Karlsruhe time-of-flight spectrometer indicated that dead time effects were overcompensated in some of our earlier measurements.

The table in fig. 19 shows some resonance peak position determinations done independently at Wisconsin, Oak Ridge, and Karlsruhe. As the sources of error are entirely different for the three measurements, the good agreement is particularly significant. A comparison of some recently measured cross sections of iron in the region between 0.5 - 0.7 MeV is shown in fig. 20. Good agreement was observed between the Karlsruhe and the GAA data. The iron data of Smith are less resolved than our data. In addition there is a systematic shift of about 5 keV, indicated by the arrows, but a shift of this amount does not represent an actual disagreement. In the Argonne data an uncertainty of several keV is quoted for the absolute energy scale.

In the case of scattering data the uncertainties associated with the individual cross section measurements are complex composites of statistical and experimental effects and often have to be estimated subjectively [35]. This, especially, is true for the inelastic scattering cross sections. Typical estimated uncertainties for elastic and inelastic scattering cross sections are quoted to be about 5 and 10 %, respectively. A recent comparison of avail-

able elastic and inelastic scattering cross sectionsfor six nuclei between C and Co was made by Perey and coworkers at Oak Ridge [31]. As an example in fig. 21 some results obtained for Fe are shown. With some exceptions there is general agreement for the total elastic and the total inelastic cross sections from different laboratories. For inelastic scattering cross sections only very few measurements have been published in overlapping energy regions.

The accuracy with which neutron reaction cross sections can be determined depends on several factors. The statistical accuracy may be quite poor applying direct counting of charged particles, while in activation measurements sufficient counting rates can be obtained. In the latter case the experimental uncertainty is largely governed by factors such as the seperation of different half lifes, the determination of the detector efficiency or the knowledge of decay schemes. Presently reported cross sections measured by the activation method quote several precent average total uncertainty in favourable cases inclusive of uncertainties in the reference standard cross section.

7. CONCLUSION

In the last few years a large amount of cross section data have been measured which could not all be mentioned here. There have been large advances in the resolution and precision by both, the improvements of existing facilities and the installation of new efficient fast neutron spectrometers. In addition there are advances in the precision of standard cross sections such as the (n,p) scattering cross section and the $^{10}B(n,\alpha)$ reaction cross section. In the field of neutron scattering cross sections a fundamental change is visible: Experimentally the measurers are going to make the transition from the knowledge of a few cases to a more systematic study of scattering processes. All activities in the fast neutron area show promise of not only quantities of cross sections, but also better fundamental understanding of nuclear reactions. Much activity is presently devoted to the use of linear accelerators and cyclotrons in nearly all fields of fast neutron cross section measurements. Several technological improvements may also be expected from new aspects and developments in the area of data processing and data acquisition. A consideration of all these facts may indicate, that the users and evaluators will be supplied with a large amount of further and more precise data. I have, however, some doubt, that it will be always exactly the data and the precision,

which is wanted by the users. In any case I know as an experimentalist, that the measurers will do their best, to satisfy the request as closely as possible.

FIGURE CAPTIONS

Fig. 1 Typical neutron spectra obtained with

a) an electron linear accelerator
b) a 140 MeV proton cyclotron
c) an isochronous cyclotron

Fig. 2 Arrangement of the time-of-flight spectrometer used with the Karlsruhe isochronous cyclotron

Fig. 3 Total neutron cross sections of oxygen measured at Karlsruhe

Fig. 4 Total neutron cross sections of iron measured by Carlson [9] at GGA

Fig. 5 Total neutron cross section data obtained by Carlson and Barshall [12]

Fig. 6 a) Measured total neutron cross sections of iron
b) Averaged total neutron cross section data of Cabé et al. [13]

Fig. 7 Comparison of total neutron cross section values with the predictions of the optical model, ref. [16]

Fig. 8 Comparison of total neutron cross section values with the predictions of the optical model, ref. [18]

Fig. 9 (n p) scattering cross sections between 1,5 and 15 MeV [25]

Fig. 10 Time-of-flight facility for fast neutron scattering experiments [35]

Fig. 11 a) Some neutron scattering data on vanadium obtained by A.B. Smith [35]
b) Inelastic scattering cross sections of ^{51}V for the excitation of the .32 and .93 MeV levels

Fig. 12 Comparison of experimental results with the calculations from the intermediate optical model [35]

Fig. 13 a) Excitation function for the 376 keV level in ^{45}Sc [37]
b) Decay scheme of ^{45}Sc

Fig. 14 a) Arrangement of the time-of-flight spectrometer at GGA
b) γ-ray spectrum from (n,xy)-reactions in oxygen [4]

Fig. 15 Excitation functions for reaction cross sections of Si [44]

Fig. 16 Cross section for the $^{10}B(n,\alpha\gamma)$-reaction up to 4,5 MeV [49]

Fig. 17 Excitation functions for reaction cross sections of
a) Ni (n,p) ref. [43]
b) ^{27}Al (n,α) ref. [46]

Fig. 18 Experimentally measured (n,2n) reaction cross sections plotted against neutron excess of the residual nuclei [51]

Fig. 19 Table giving some resonance peak positions determined at Wisconsin, Oak Ridge and Karlsruhe

Fig. 20 Comparison of recent iron total cross section data [11]

Fig. 21 Comparison of elastic and inelastic cross sections for iron [31]

REFERENCES

[1] Lopez, W.M., Friesenhahn, S.J., Fröhner, F.H., Report GA-7820 (1967).

[2] Cierjacks, S., Duelli, B., Forti, P., Kopsch, D., Kropp, L., Lösel, M., Nebe, J., Schweickert, H., Unseld, U., Rev. Sci. Instr. 39 (1968) 1279.

[3] Carlson, A.D., private communication.

[4] Orphan, V.J., Hoot, C.G., Carlson, A.D., John, J., Beyster, J.R., Nucl. Instr. Meth. 73 (1969) 1.

[5] Kropp, L., Forti, P., Report KFK 1190 to be published.

[6] Yergin, P.F., Martin, R.C., Winhold, E.J., Medicus, H.A., Moyer, W.R., Augustson, R.H., Kaushal, N.N., Fullwood, R.R., Neutron Cross Sections and Technology (Proc. Conf. Washington D.C., March 1966) CONF.-660303 (1966) 690.

[7] Rössle, E., Tauber, M., Nuclear Structure Study with Neutrons (Proc. Conf. Antwerp, 1965) North-Holland Publishing Company, Amsterdam (1966) 281.

[8] Stüwer, D., Genz, H., Bormann, M., Nucl. Phys. 62 (1965) 165.

[9] Carlson, A.D., private communication.

[10] Davis, J.C., Noda, F.T., Nucl. Phys. A 134 (1969) 361.

[11] Cierjacks, S., Report EANDC (E) 122 "AL" (1969).

[12] Carlson, A.D., Barshall, H.H., Phys. Rev. 158 (1967) 1142.

[13] Cabé, J., Laurat, M., Yvon, P., Bardolle, G., Nucl. Phys. A 102 (1967) 92.

[14] Cabé, J., Report CEA-R 3279 (1967).

[15] Feshbach, H., Kerman, A.K., Lemmer, R.H., Ann. Phys. 41 (1967) 230.
Farrel, J.A., Kyker, G.C., Bilpuch, E.G., Newson, H.W., Phys. Lett. 17 (1965) 286.
Monahan, J.E., Elwyn, A.J., Nucl. Phys. A 123 (1969) 33.
Bowman, C.D., Bilpuch, E.G., Newson, H.W., Ann. Phys. 17 (1962) 319.
Lejenne, A., Mahaux, C., Z. Phys. 207 (1967) 35.

[16] Glasgow, D.W., Foster, Jr., D.G., Phys. Rev. Lett. 22 (1969) 139.

[17] Perey, F., Buck, B., Nucl. Phys. 32 (1962) 353.

[18] Cierjacks, S., Nebe, J., Tsien, T., Optical Model Analysis of Total Neutron Cross Sections, publication in progress.

[19] de Villiers, J.A.M., Engelbrecht, C.A., Vonach, W.G., Smith, A.B., Z. Phys. 183 (1965) 323.

[20] Vonach, W.G., Smith, A.B., Moldauer, P.A., Phys. Lett. 11 (1964) 331.

[21] Engelbrecht, C.A., Fiedeldey, H., Ann. Phys. 42 (1967) 262.

[22] Lane, A.M., Lynn, J.E., Melkonian, E., Rae, E.R., Phys. Rev. Lett. 2 (1959) 424.

[23] Moldauer, P.A., Nucl. Phys. 47 (1963) 65.

[24] Hrehuss, G., Czibók, T., Phys. Lett. 28 B (1969) 585.

[25] Schwartz, R.B., Schrack, R.A., Heaton, H.T., Phys. Lett. 30 B (1969) 36.

[26] Clements, P.J., Langsford, A., Phys. Lett. 30 B (1969) 25.

[27] Clements, P.J., Langsford, A., Report, AERE-PR/NP 16, (1970)

[28] Cierjacks, S., Forti, P., Kirouac, G.J., Kopsch, D., Kropp, L., Nebe, J., Phys. Rev. Lett. 23 (1969) 866.

[29] Tsukada, K., Tanaka, S., Tomita, Y., Maruyama, M., Nucl. Phys. A 125 (1969) 641.

Maruyama, M., Nucl. Phys. A 131 (1969) 145.

Kikuchi, S., Yamamuti, Y., Nishimura, K., J. Phys. Soc. Japan 28, 4 (1970) in press.

[30] Menlove, H.O., Coop, K.L., Grench, H.A., Phys. Rev. 163 (1967) 1299.

[31] Perey, F.G., private communication.

[32] Smith, A.B., Whalen, J.F., Barnard, E., de Villiers, J.A.M., Report ANL-7636 (1969) and to be published in Nucl. Sci. and Eng.

Barnard, E., de Villiers, J.A.M., Engelbrecht, C.A., Reitmann, D., Nucl. Phys. A 118 (1968) 321.

[33] Holmquist, B., Wiedling, T., Report AE-366 (1969).

Holmquist, B., Arkiv för Fysik, 38 25 (1968) 403.

Holmquist, B., Johannsson, S.G., Lodin, G., Wiedling, T., Report AE-375 (1969).

[34] Holmquist, B., Johannsson, S.G., Lodin, G., Salama, M., Wiedling, T., Report AE-385 (1969).

[35] Smith, A.B., Whalen, J.F., Takeuchi, K., Report ANL-7564 (1969) and to be published in Phys. Rev.

[36] Holmquist, B., Wiedling, T., Neutron Cross Sections and Technology (Proc. Conf. Washington D.C., March 1968), NBS Special Publication 299 (1968) 845.

[37] Rogers, V.C., Beghian, L.E., Clikeman, F.M., Nucl. Phys. A 137 (1968) 85.

[38] Bormann, M., Dreyer, F., Seebeck, U., Voigts, W., Z. Naturforschung 21 A (1966) 988.

[39] Vonach, H.K., Vonach, W.G., Neutron Cross Sections and Technology (Proc. Conf. Washington D.C., March 1968), NBS Special Publication 299 (1968) 885.

[40] Colli, L., private communication to the CCDN Saclay (1969).

[41] Ranakumar, R., Kondaiah, E , Fink, R.W., Nucl. Phys. A 122 (1968) 679.
Tiwari, P.N., Kondaiah, E., Phys. Rev. 167 (1968) 1091.

[42] Csikai, J., Atomki Közl. 8 (1966) 79

[43] Paulsen, A., Nukleonik 10 (1967) 91.

[44] Grimes, S.M., Nucl. Phys. A 124 (1969) 369.

[45] Bass, R., Report EANDC/E-89 (1966).
Spira, C., Robson, J.M., Nucl. Phys. A 127 (1969) 81.

[46] Schmitt, H.W., Halperin, J., Phys. Rev. 121 (1961) 827.

[47] Paulsen, A., Liskien, H., Nukleonik 8 (1966) 315.

[48] Bormann, M., Behrend, A., Riehle, I., Vogel, O., Nucl. Phys. A 115 (1968) 309.

[49] Steward, L., Report EANDC(US)-137 "A", INDC (USA)-18 "G" (1970);
Bogart, D., Nichols, L.L., Nucl. Phys. A125 (1969) 463;
Macklin, R.L., Gibbons, J.H., Phys. Rev. 165 (1968) 1147.

[50] Chatterjee, A., Nucl. Phys. 49 (1963) 686; Nucl. Phys. 60 (1964) 273.

[51] Chatterjee, S., Chatterjee, A., Nucl. Phys. A 125 (1969) 593.

[52] Schmidt, J.J., Report KFK 120 (EANDC-E-35U) (1966)

[53] Cierjacks, S., Forti, P., Kopsch, D., Kropp, L., Nebe, J., Unseld, H.,
Report KFK 1000 (EUR 3963e, EANDC (E)-111 "U") (1968).

[54] Johnson, C.H., Haas, F.H., Fowler, J.L., Martin, F.D., Kernell, R.L.,
and Cohn, H.O., Neutron Cross Sections and Technology (Proc. Conf.,
Washington D.C., March 1968), NBS Special Publication 299 (1968) 851.

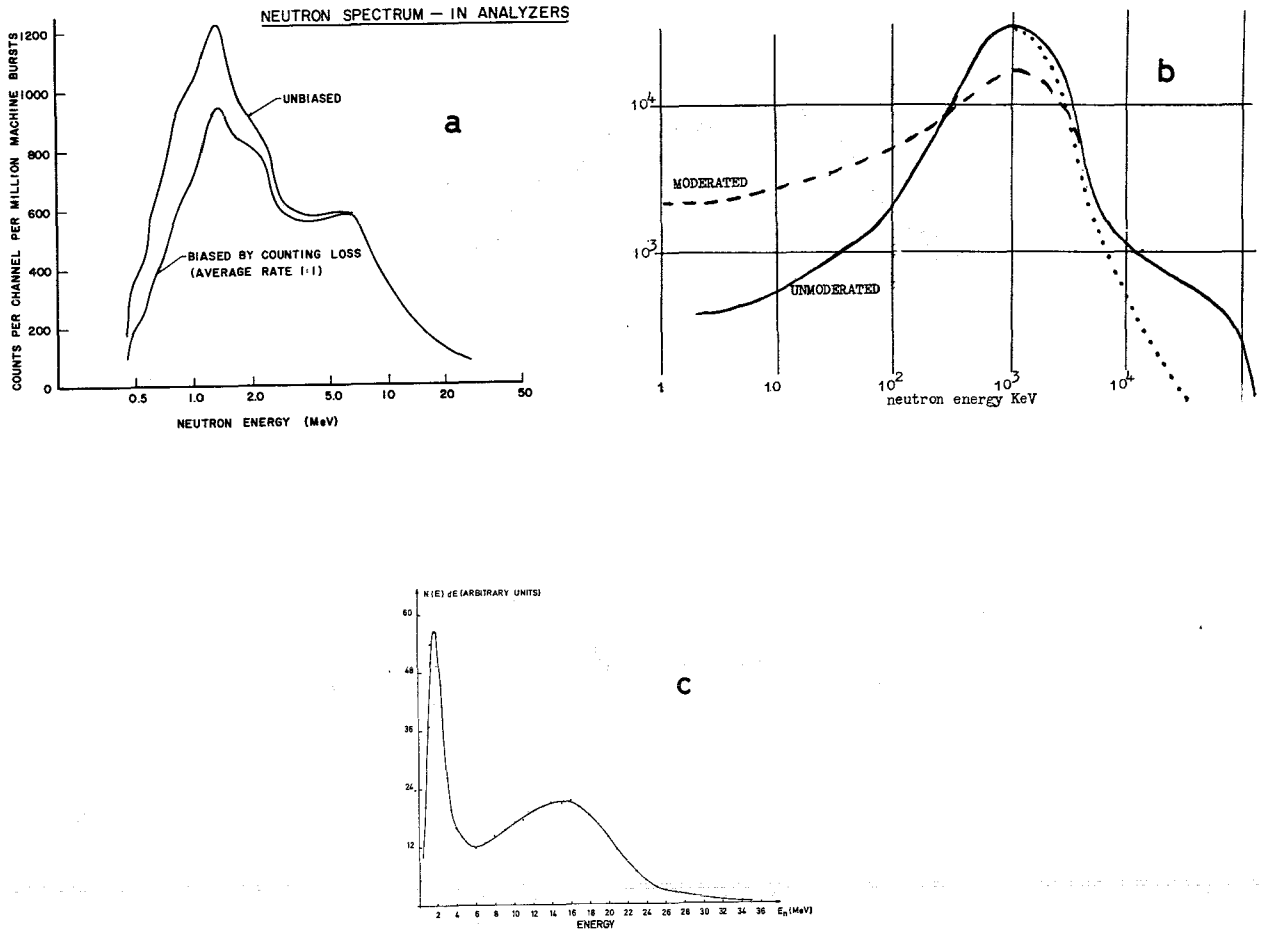
NEUTRON SPECTRUM — IN ANALYZERS
COUNTS PER CHANNEL PER MILLION MACHINE BURSTS
UNBIASED
BIASED BY COUNTING LOSS (AVERAGE RATE 1:1)
a
NEUTRON ENERGY (MeV)
b
MODERATED
UNMODERATED
neutron energy KeV
c
ENERGY

Fig. 1

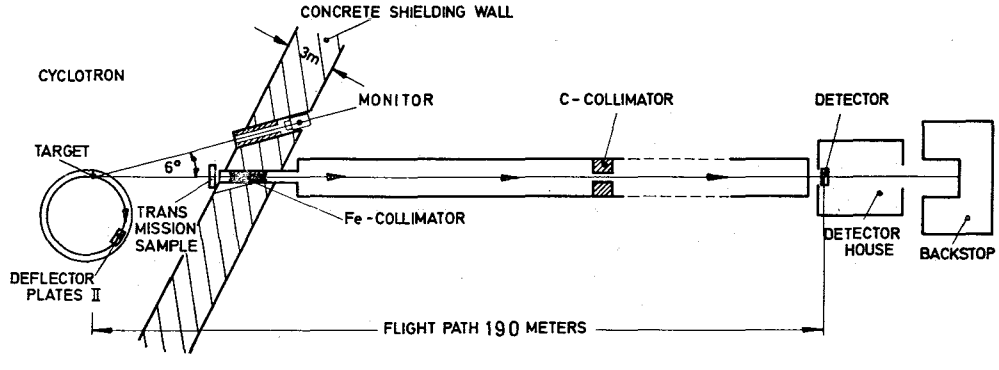
CONCRETE SHIELDING WALL
3m
CYCLOTRON
MONITOR
C-COLLIMATOR
DETECTOR
TARGET
6°
TRANS MISSION SAMPLE
Fe-COLLIMATOR
DETECTOR HOUSE
BACKSTOP
DEFLECTOR PLATES II
FLIGHT PATH 190 METERS

Fig. 2

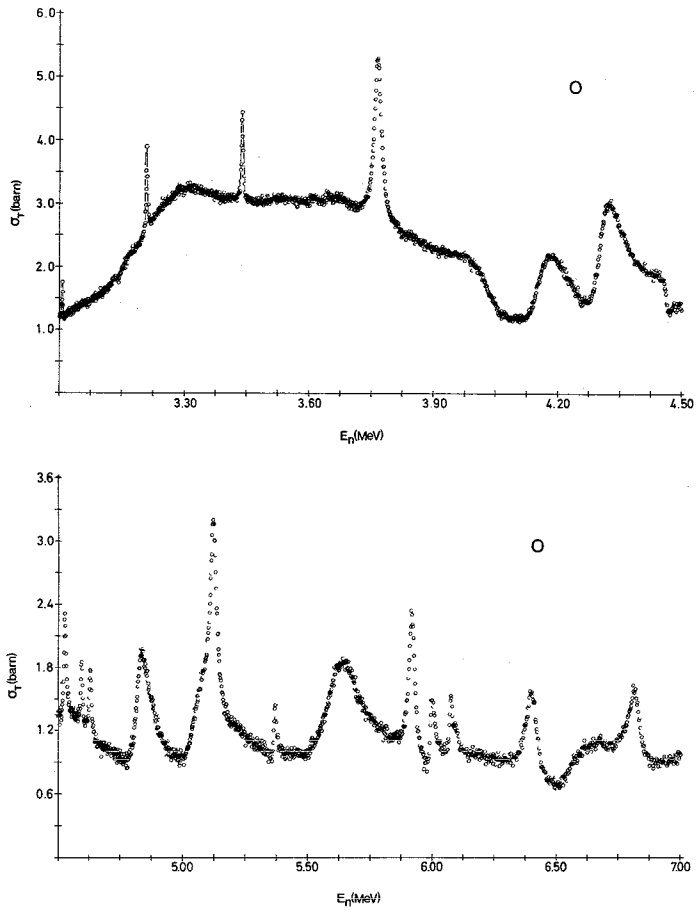
O
σ_t (barn)
E_n(MeV)
O
σ_t (barn)
E_n(MeV)

Fig. 3

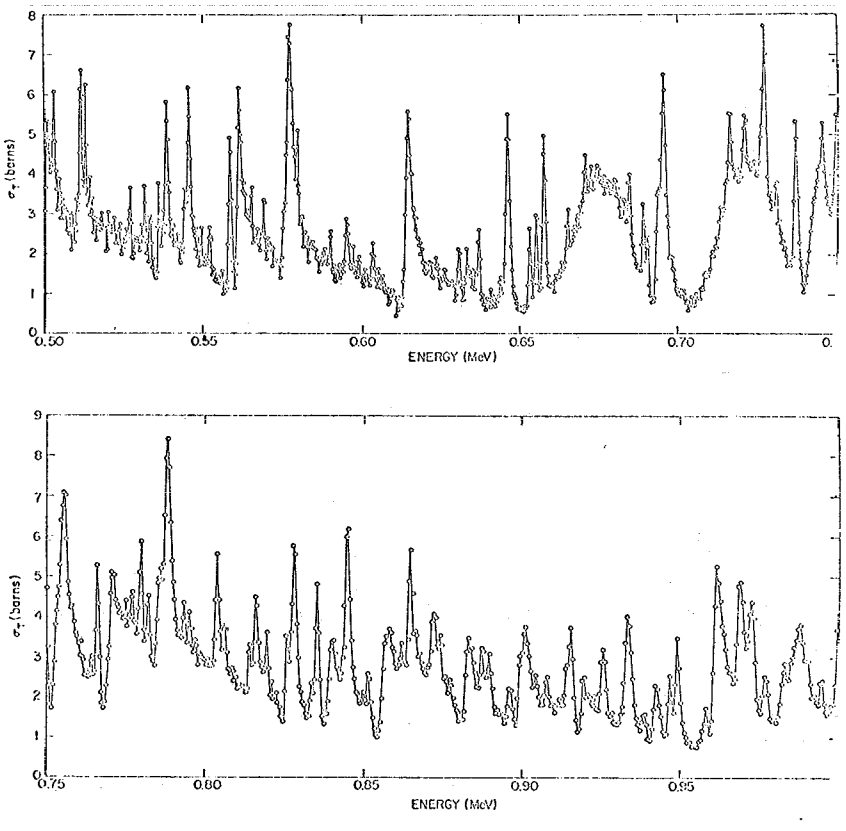
σ_t (barns)
ENERGY (MeV)
σ_t (barns)
ENERGY (MeV)

Fig. 4

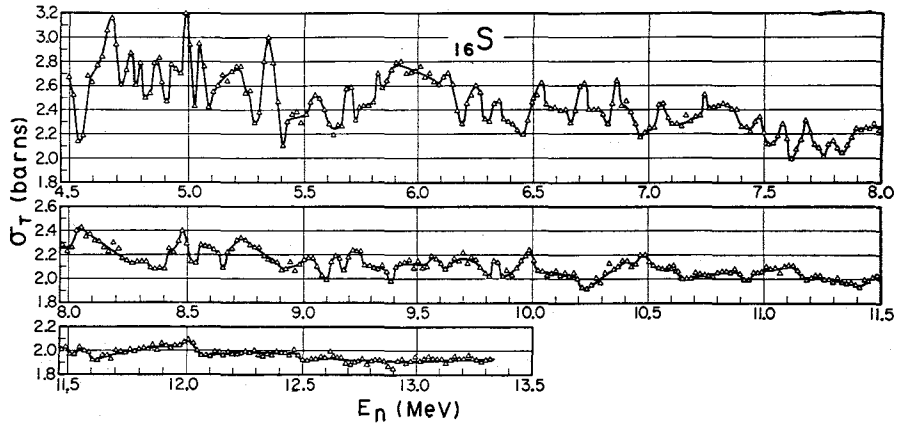

Fig. 5

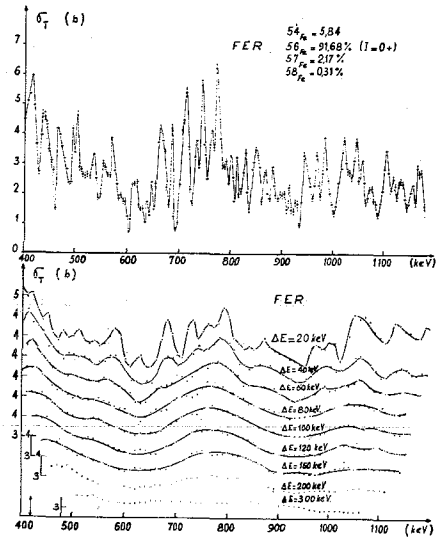

Fig. 6

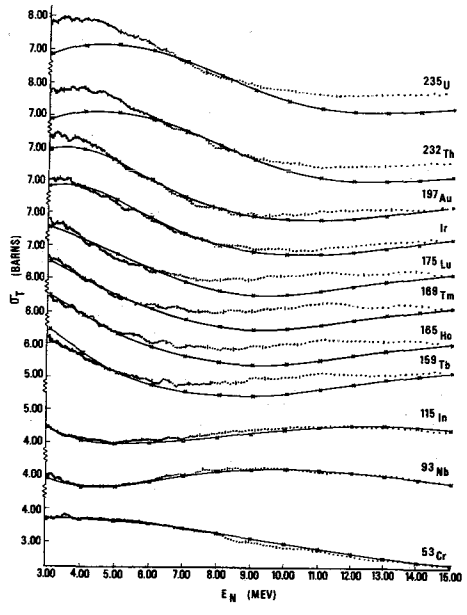

Fig. 7

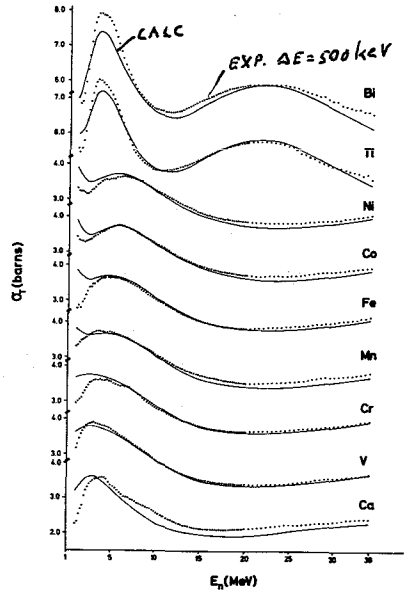

Fig. 8

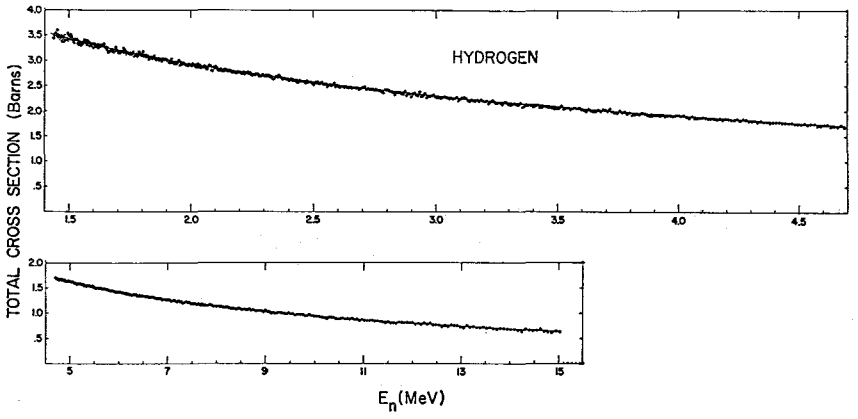

Fig.9

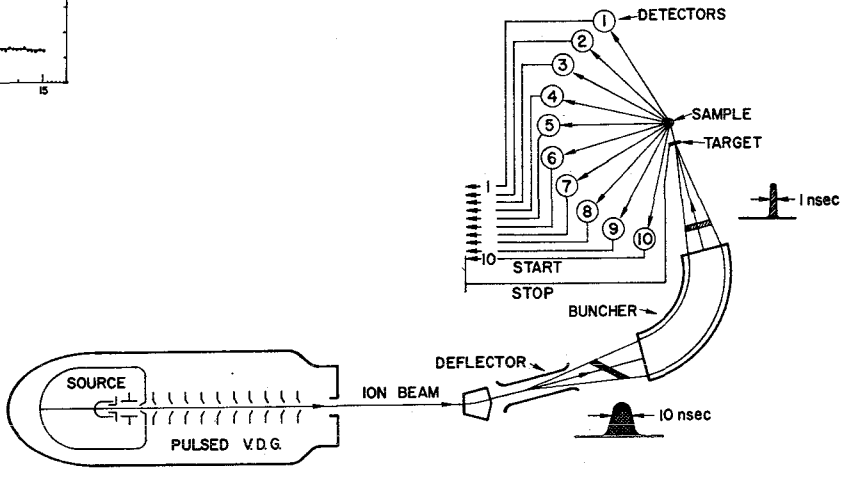

Fig.10

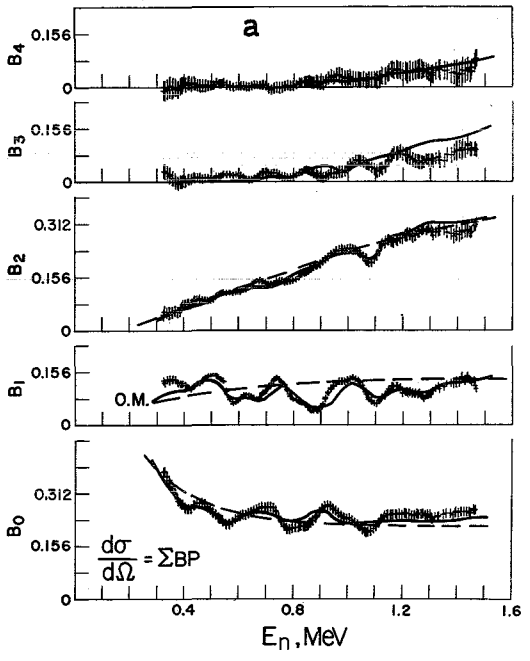

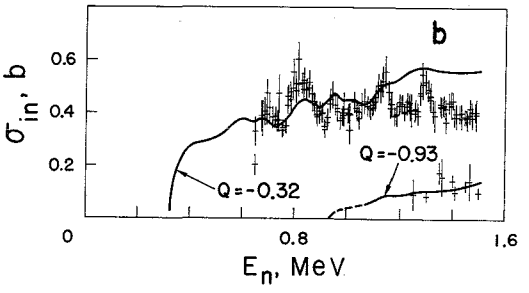

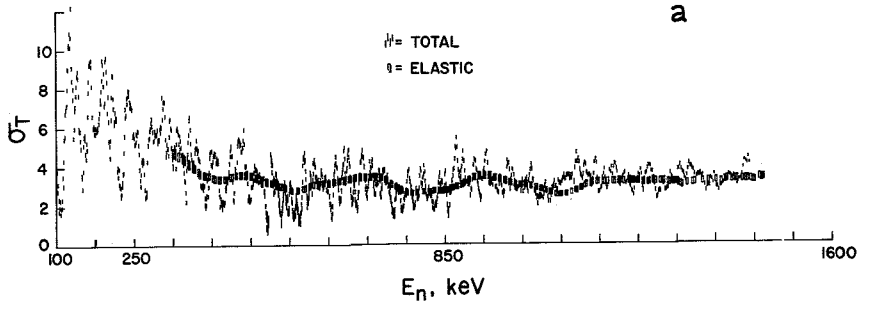

Fig.11

Real (V) and Imaginary (W) Portions of the Intermediate Optical Potential (Eq. 20), Calculated, Compared with the Phenomenological Optical Potential Derived from a Fit to the Measured Elastic Scattering Distributions, EXP. Positions of doorway states are indicated by arrows referring to Table IV values.

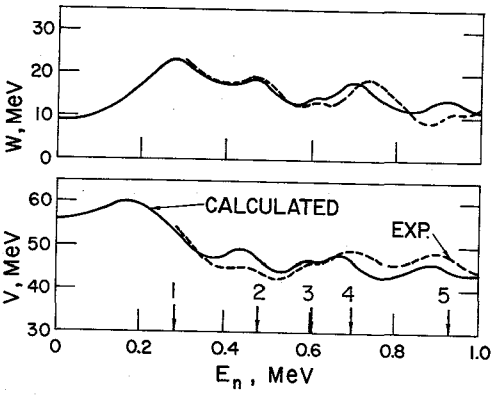

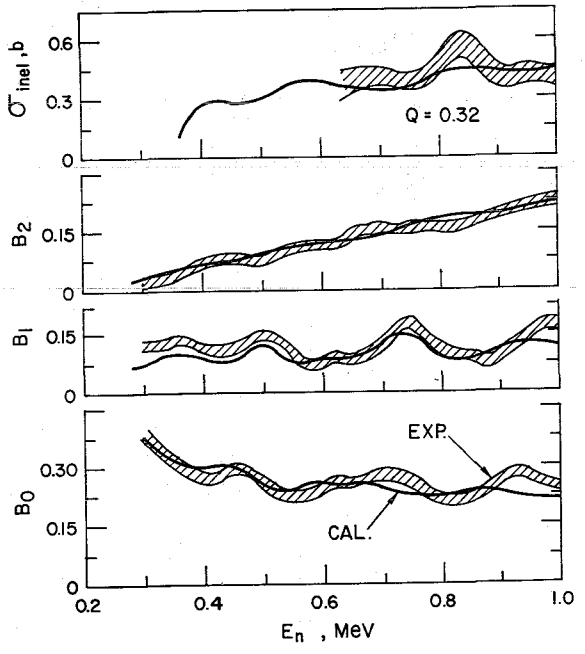

Comparison of Experimental Elastic Scattering Angular Distributions and Inelastic Cross Sections, EXP., of Vanadium with Those Calculated from the Intermediate Optical Potential and Statistical Theory, CAL.

Fig.12

b

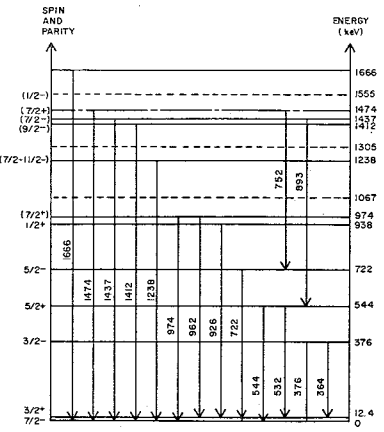

a

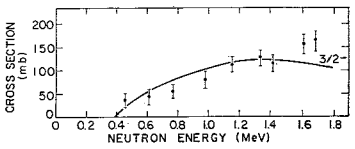

Fig. 13

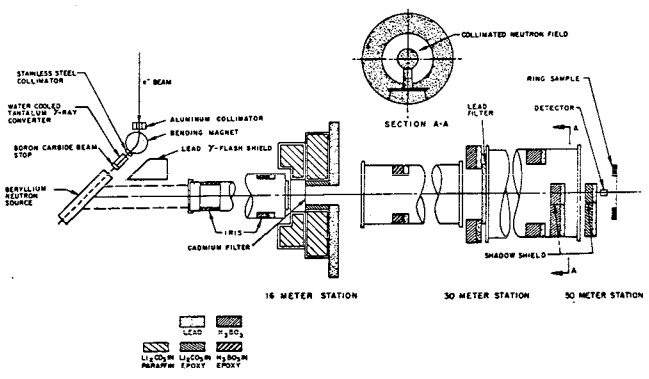

Fig. 14 a

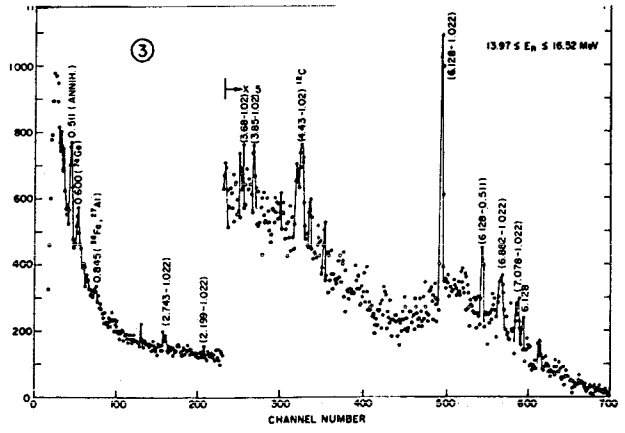

Fig. 14 b

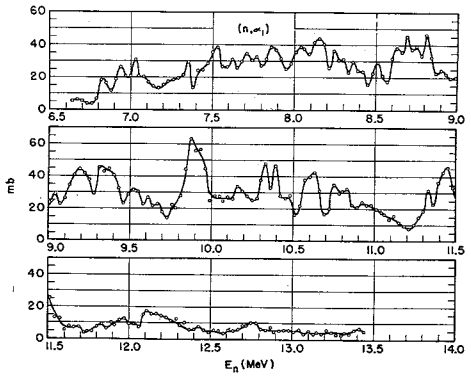

Fig. 15 a

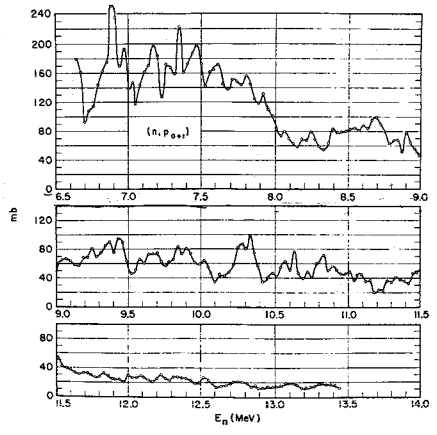

Fig. 15 b

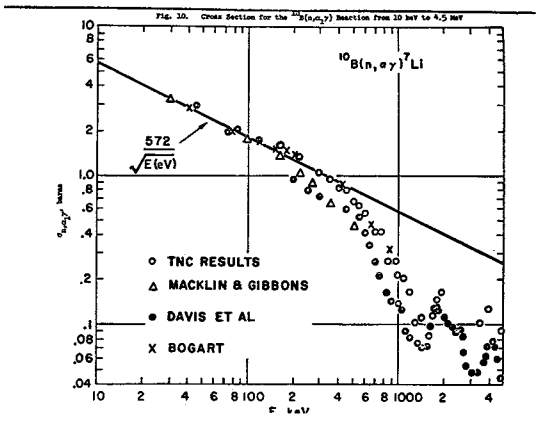

Fig. 16

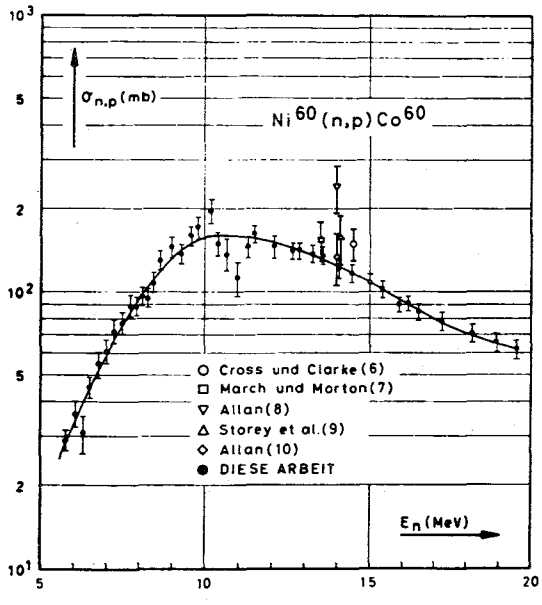

Fig.17a

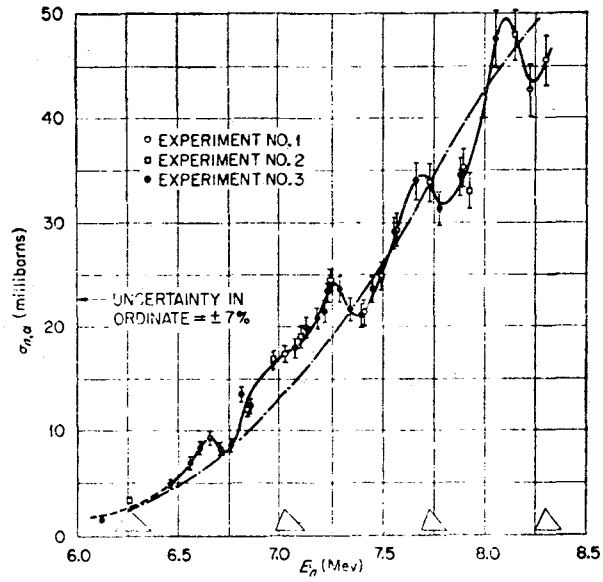

Fig. 17 b

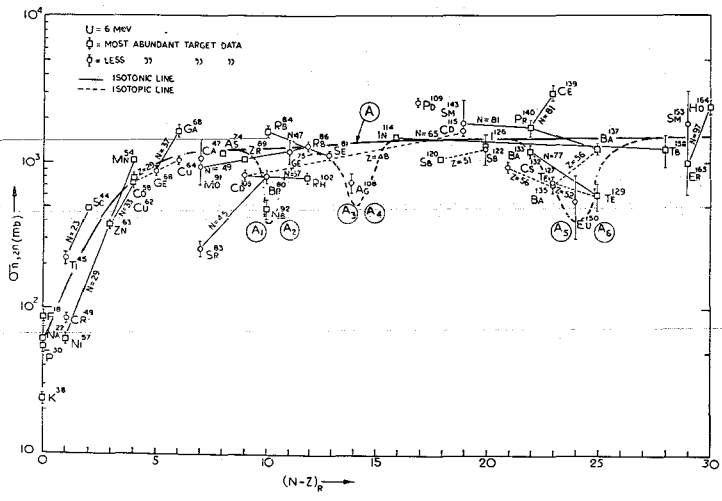

Fig.18

Fig.19

Resonance peak positions (keV)

Cierjacks et al. [53]	Davis and Noda [10]	Johnson et al. [54]
	Carbon	
4933 ± 5	4935 ± 4	
5369 ± 6	5368 ± 5	
6293 ± 8	6294 ± 5	
7755 ± 11	7759 ± 8	
	Oxygen	
1651 ± 1		1651 ± 2
1690 ± 1		1689 ± 2
1833 ± 1		1833 ± 2
1906 ± 1		1906 ± 2
2352 ± 2		2353 ± 2
3211 ± 3		3213 ± 2
3440 ± 3		3443 ± 2
3765 ± 4	3765 ± 3	
5122 ± 4	5122 ± 4	
5906 ± 7	5914 ± 5	
6386 ± 8	6395 ± 7	
6806 ± 9	6807 ± 7	
7193 ± 9	7200 ± 8	

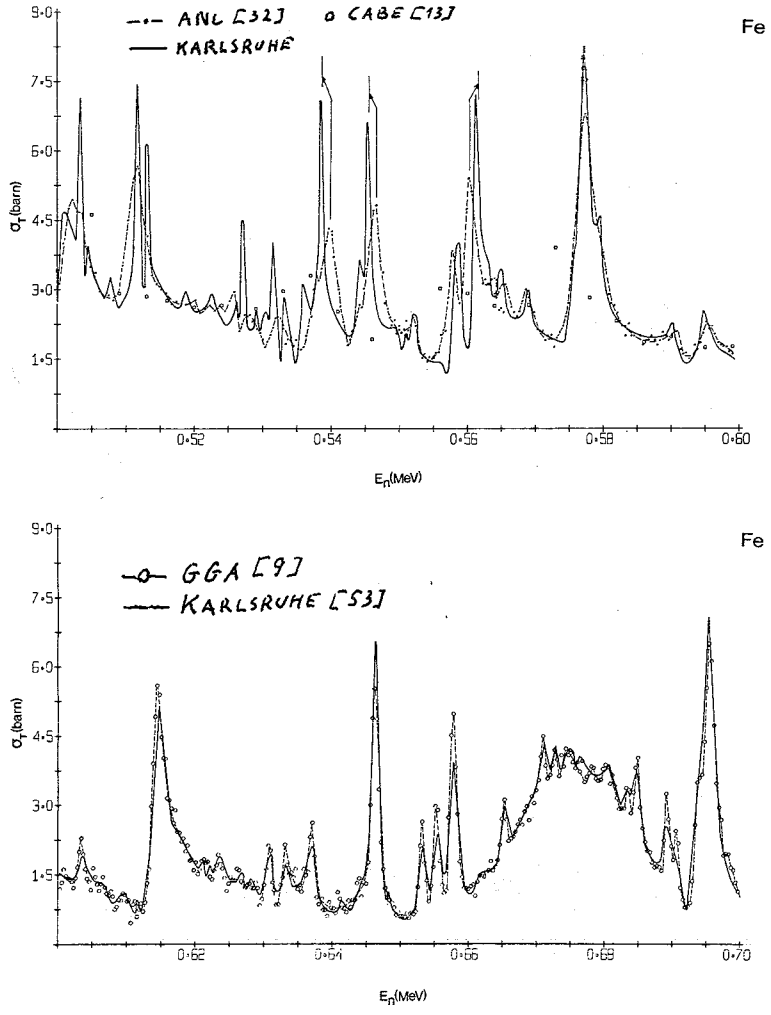
ANL [32]
CABE [13]
KARLSRUHE
Fe
σ_t(barn)
E_n(MeV)
GGA [9]
KARLSRUHE [53]
Fe
σ_t(barn)
E_n(MeV)

Fig. 20

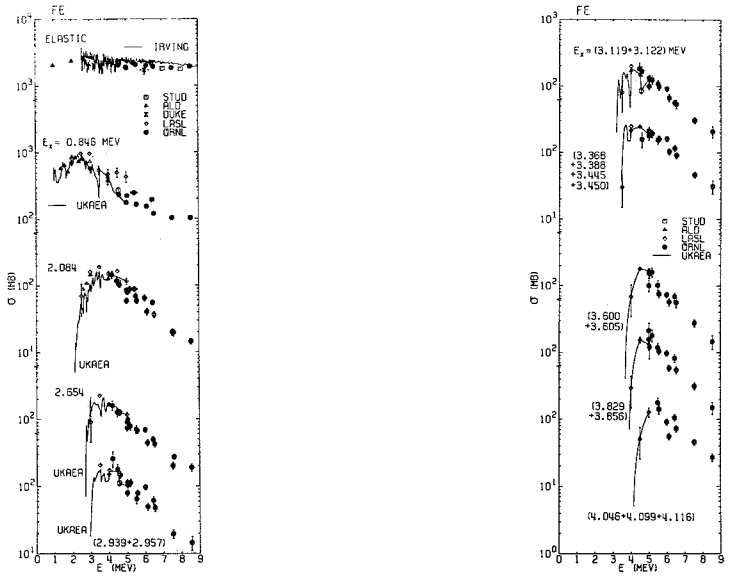
FE
ELASTIC
IRVING
STUD
ALO
DUKE
LASL
ORNL
E_x = 0.846 MEV
UKAEA
2.084
UKAEA
2.654
UKAEA
UKAEA
(2.939+2.957)
σ (MB)
E (MEV)
FE
E_x = (3.119+3.122) MEV
(3.368
+3.388
+3.445
+3.450)
STUD
ALO
LASL
ORNL
UKAEA
(3.600
+3.605)
(3.829
+3.856)
(4.046+4.099+4.116)
σ (MB)
E (MEV)

Fig. 21